Electronic Supplementary Material (ESI) for Lab on a Chip.

Performance Tuning of Microfluidic Flow-Focusing Droplet Generators

Ali Lashkaripour[1,2], Christopher Rodriguez[3], Luis Ortiz[1,4], and Douglas Densmore [⋆, 1,5]

[1]Biological Design Center, 610 Commonwealth Avenue, Boston, USA.
[2]Boston University Biomedical Engineering Department, Boston, USA.
[3]Department of Cyber Engineering, Louisiana Tech University, Ruston, USA.
[4]Boston University Department of Molecular Biology, Cell Biology & Biochemistry, Boston, USA.
[5]Boston University Department of Electrical and Computer Engineering, Boston, USA.

The supplementary information includes the following information to support the submission of our manuscript to ***Lab on a Chip*** journal titled "Performance Tuning of Microfluidic Flow-Focusing Droplet Generators".

- Detailed fabrication and assembly of the microfluidic device.
- Main effect analysis plots grouped based on droplet formation regimes, to enable researchers to fine-tune a droplet generator based on the observed generation regime.
- A more detailed description of role aspect ratio on droplet generation.
- 150 Experimental data point of both droplet diameter and generation rate.
- A table that provides all of the possible devices that could be used to reach a certain range of performance (i.e., a certain range of droplet diameter and generation rate).

S. 1. Device design, fabrication and assembly

The desktop CNC mill used in this study was an Othermill pro (Othermill) which cost $3200. It should be mentioned that Othermill company was bought by Bantam Tools company, and Othermill Pro CNC mill was renamed to Bantam Tools Desktop PCB Milling Machine. SolidWorks, Fusion 360, and OtherPlan software were used to realize a low-cost micro-milled chip out of polycarbonate for any given design. Through this method, each device is fabricated in less than 1 hour and costs less $10. The fabrication steps for each layer are shown in Fig. S. 1. It should be mentioned that Othermill pro delivers an accuracy of 25 μm. However, if the channel width and endmill cutting diameter are equal, accuracy improves significantly to 10 μm and less, depending on the endmill cutting diameter [1]. Therefore, all the orifices were milled out using an endmill with the same cutting diameter as the orifice width. High-precision carbide endmills (Performance Micro Tool) with diameters of 75, 100, 125, 150, and 175 μm were used in this study

⋆Corresponding author: dougd@bu.edu

to assure all the orifices are milled out as accurately as possible. The channels (i.e., oil inlet, water inlet, and outlet) were milled out using an endmill with a cutting diameter equal to the channel width if possible. If an endmill with a cutting diameter equal to the channel width was not available an endmill with a cutting diameter as close as possible to the channel width was used.

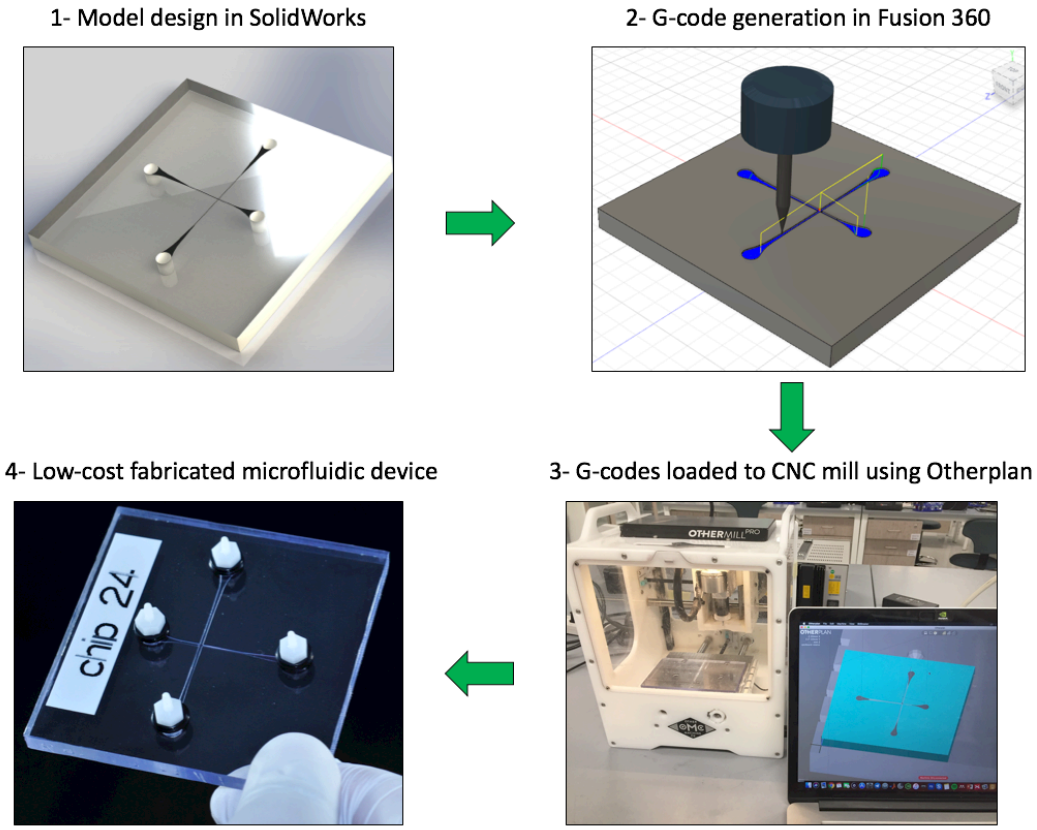

Fig. S. 1. Design-to-device steps utilized in this study to fabricate microfluidic droplet generators in a time- and cost-efficient manner. Devices are designed in SolidWorks and saved and .STEP files. These files are loaded to Fusion 360 to generate milling paths as G-codes. G-codes are loaded to the desktop micro-mill using OtherPlan. Desktop micro-milled devices can be fabricated in less than 1 hours and cost less than $10.

The microfluidic devices used in this study consist of five layers. A flow layer, a control layer, and an elastic layer sandwiched between the flow and control layers to seal the device. To improve the sealing of the device to withstand higher pressures, we milled out two layers for pressure distributors out of polycarbonate and clamped them using clamps, as shown in Fig. S. 2. The flow layer, control layer, and pressure distributors were all milled out of a polycarbonate substrate with a thickness of 5.5 mm.

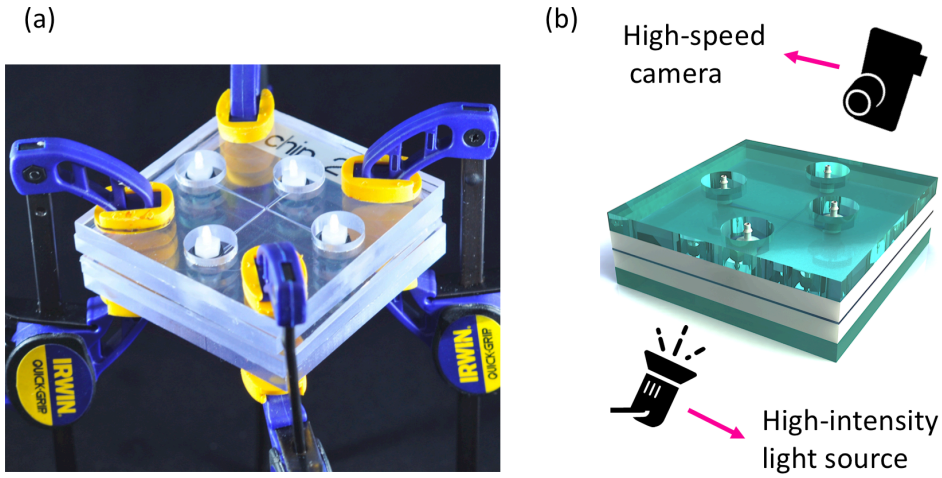

Fig. S. 2 Assembly of the microfluidic device. (a) A microfluidic droplet generator with five layers clamped down to deliver a higher sealing pressure. (b) A high-speed camera was mounted on a stereo microscope above the microfluidic chip. A high-powered LED impulse light source was placed underneath the device to enable high-speed imaging.

As shown in Fig. S. 3, the sealing is greatly improved by using pressure distributors and clamps to push down the flow and control layer against the PDMS layer. This assembly method enables a straightforward and reversible bonding protocol while keeping the bonding pressure high-enough to be suitable for a wide range of applications.

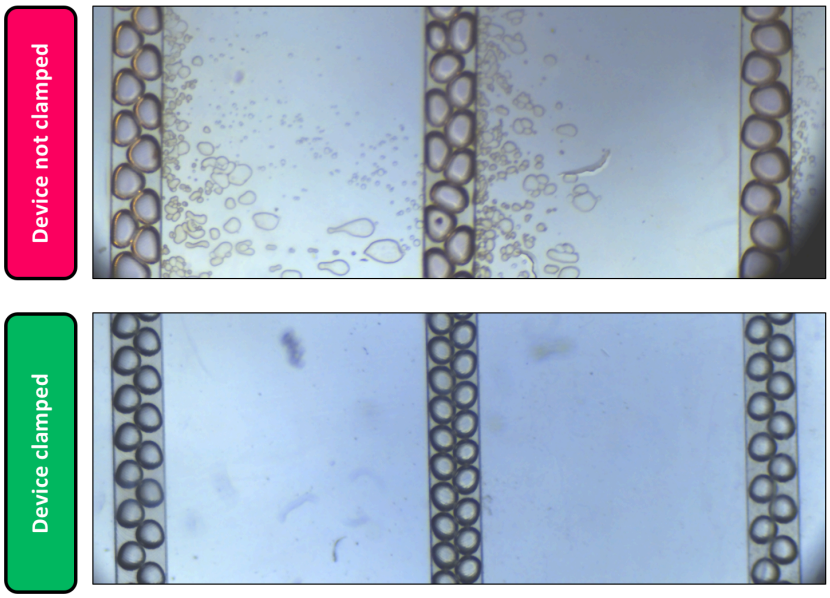

Fig. S. 3. The sealing pressure of the microfluidic device is significantly improved when pressure distributors and clamps are used. As shown in the figure, devices with no pressure distributors and clamps are prone to fluid leakage from the microchannels to the space between the flow layer and the PDMS layer. On the other hand, devices with pressure distributors and clamps showed no sign of leakage even at higher flow rates.

S. 2. Performance tuning in the dripping regime

In here, we provide the main effect analysis for all the data observed in the dripping regime (i.e., 361 data points) required for performance tuning of flow-focusing droplet generators at the dripping regime. Fig. S. 4 shows how changing each one of the eight input parameters (while keeping the other parameters constant) alters the observed droplet diameter in the dripping regime.

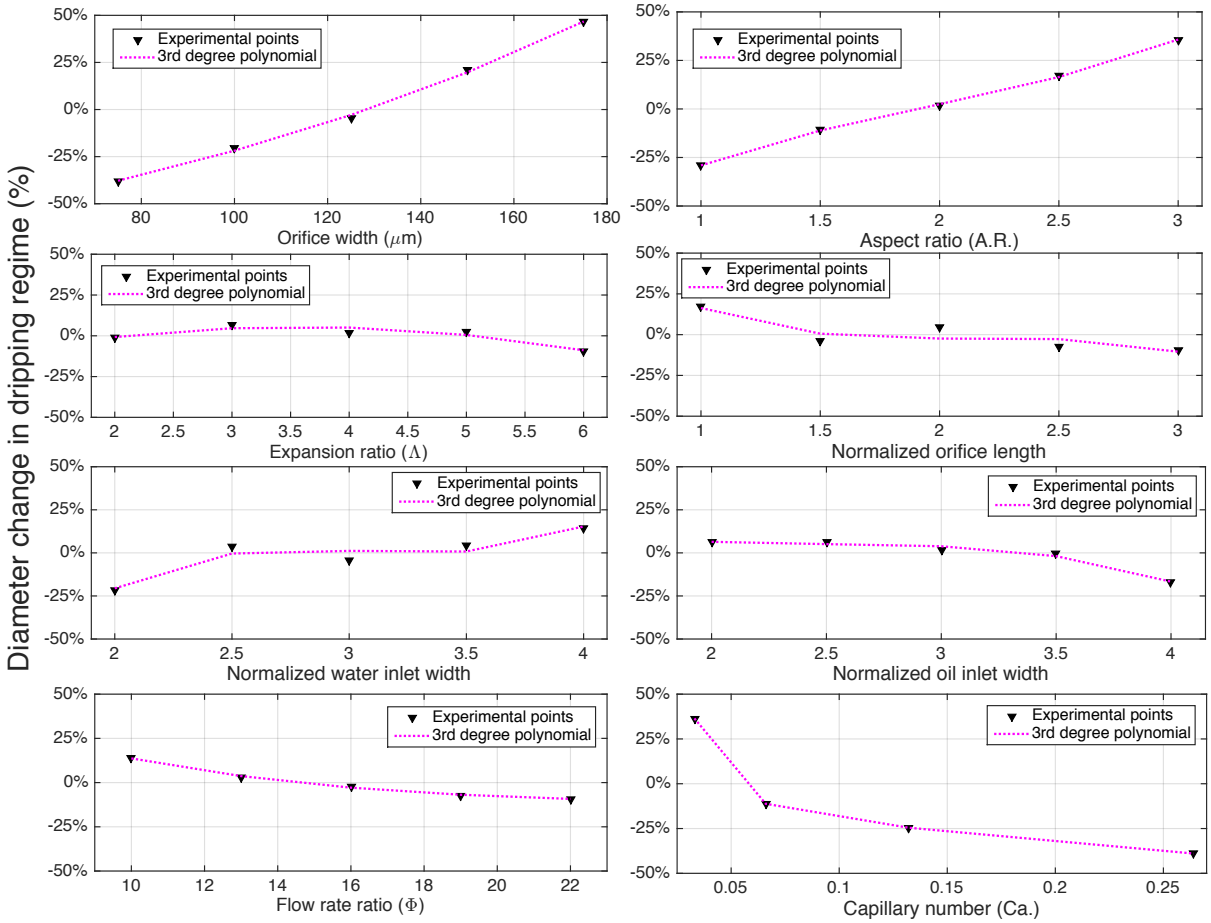

Figure S. 4 Main effect plots of droplet diameter in the dripping regime. This demonstrates how changing an input parameter while keeping the others constant will on average change the droplet diameter. These plots are generated based on 361 data points obtained in the dripping regime with an average droplet diameter of 108.1 µm.

In Fig. S. 5 the main effect analysis for generation rate in dripping regime is given. This figure shows how changing each one of the eight input parameters (while keeping the other parameters constant) alters the observed generation rate in the dripping regime.

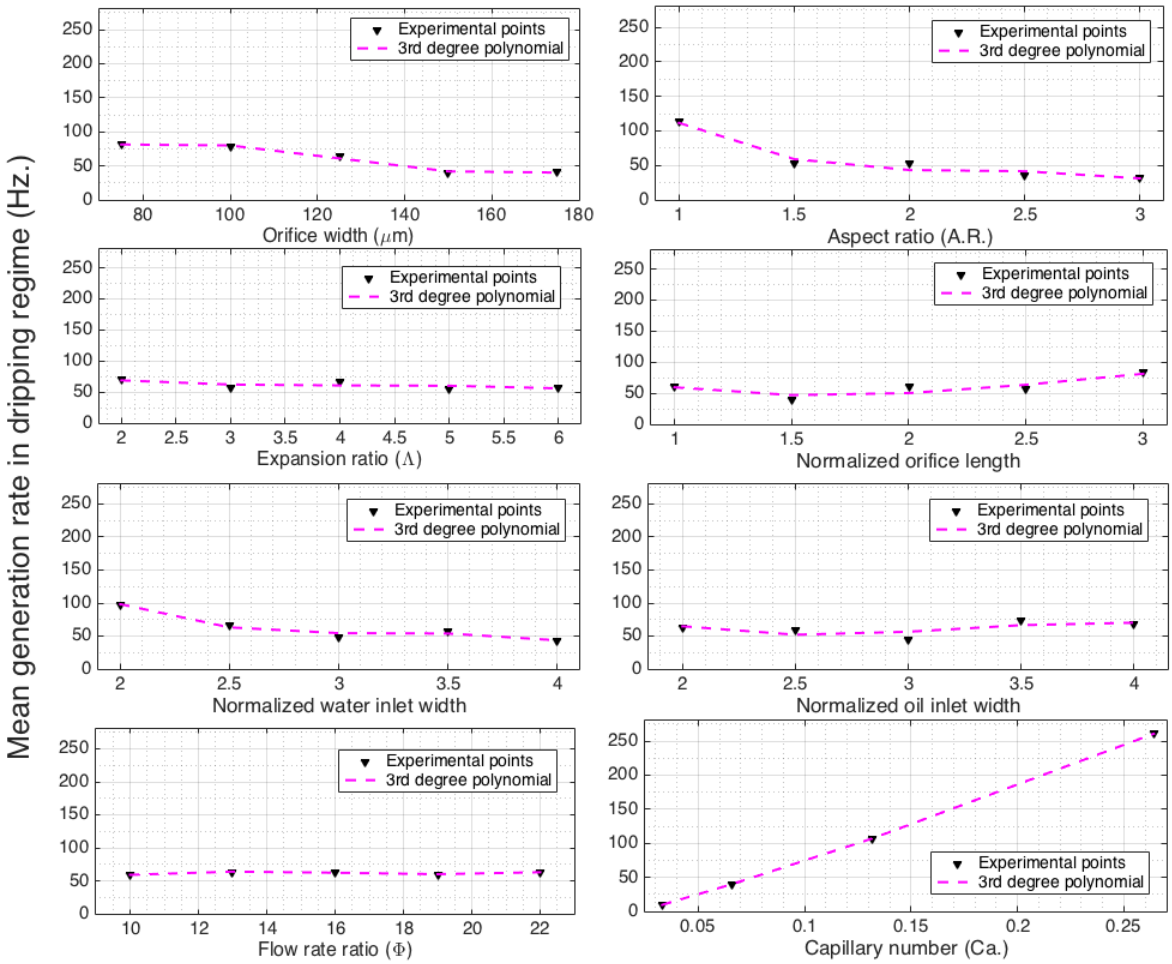

Figure S. 5 Main effect plots of droplet generation rate in dripping regime. This demonstrates how changing an input parameter while keeping the others constant will on average change the generation rate. These plots are generated based on 361 data points obtained in the dripping regime with an average generation rate of 61.6 Hz. Researchers can normalize these plots by the average generation rate to translate generation rate variations to percentage change in the observed droplet generation rate.

S. 3. Performance tuning in the jetting regime

In here, we provide the main effect analysis for all the data observed in the jetting regime (i.e., 389 data points) required for performance tuning of flow-focusing droplet generators at the jetting regime. Fig. S. 6 shows how changing each one of the eight input parameters (while keeping the other parameters constant) alters the observed droplet diameter in the jetting regime.

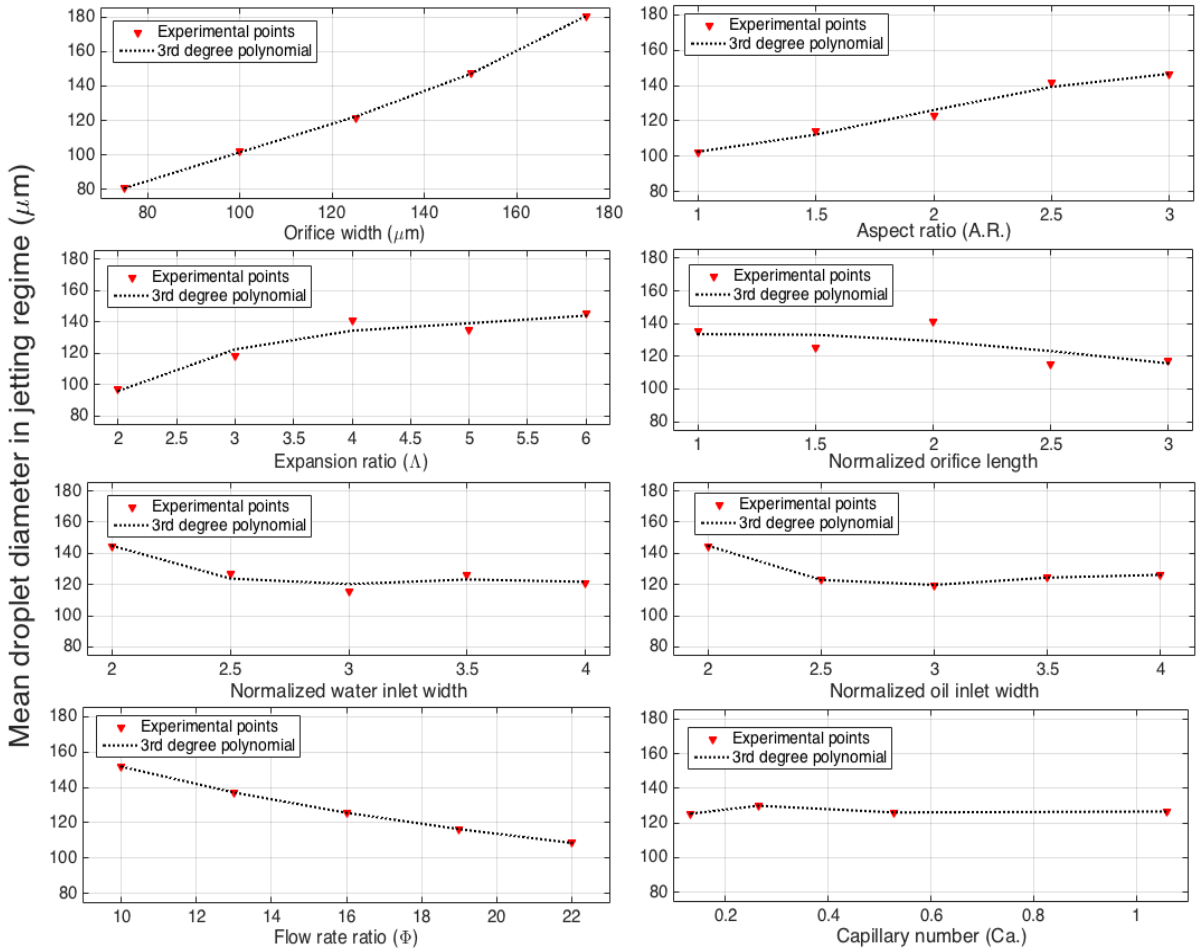

Figure S. 6 Main effect plots of droplet diameter in the jetting regime. This demonstrates how changing an input parameter while keeping the others constant will on average change the droplet diameter. These plots are generated based on 389 data points obtained in the jetting regime with an average droplet diameter of 126.9 µm. Researchers can normalize these plots by the average droplet diameter to translate diameter variations to percentage change in droplet size.

Fig. S. 7 shows how changing each one of the eight input parameters (while keeping the other parameters constant) alters the observed generation rate in the jetting regime.

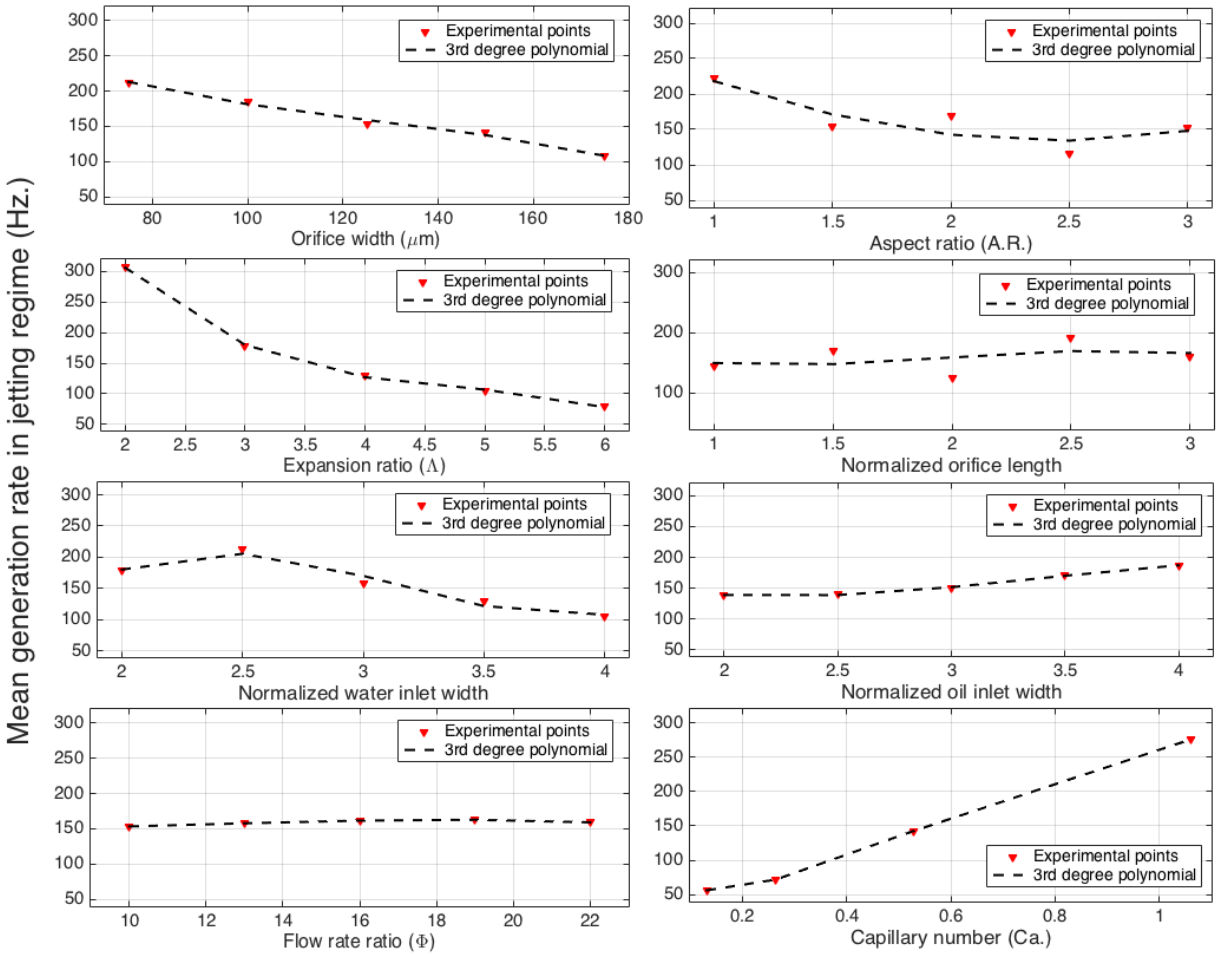

Figure S. 7 Main effect plots of droplet generation rate in the jetting regime. This demonstrates how changing an input parameter while keeping the others constant will on average change the generation rate. These plots are generated based on 389 data points obtained in the jetting regime with an average generation rate of 158.5 Hz. Researchers can normalize these plots by the average generation rate to translate rate variations to percentage change in droplet generation rate.

S. 4. Effect of aspect ratio on generation regime

The aspect ratio plays a major role at medium capillary numbers (i.e., $Ca. = 0.13 - 0.53$), in generation rate, droplet diameter, polydispersity, and generation regime, as discussed in sections 3.1 - 3.4 of the manuscript. To clarify the importance of aspect ratio in determining droplet formation regime (that results in changes in generation rate, droplet diameter, and droplet polydispersity), we show experimental snapshots of droplet formation for all the devices with an aspect ratio of 1, 1.5, and 2 at a constant flow condition (i.e., $Ca. = 0.264$ & $\Phi = 16$.) in Fig. S. 8.

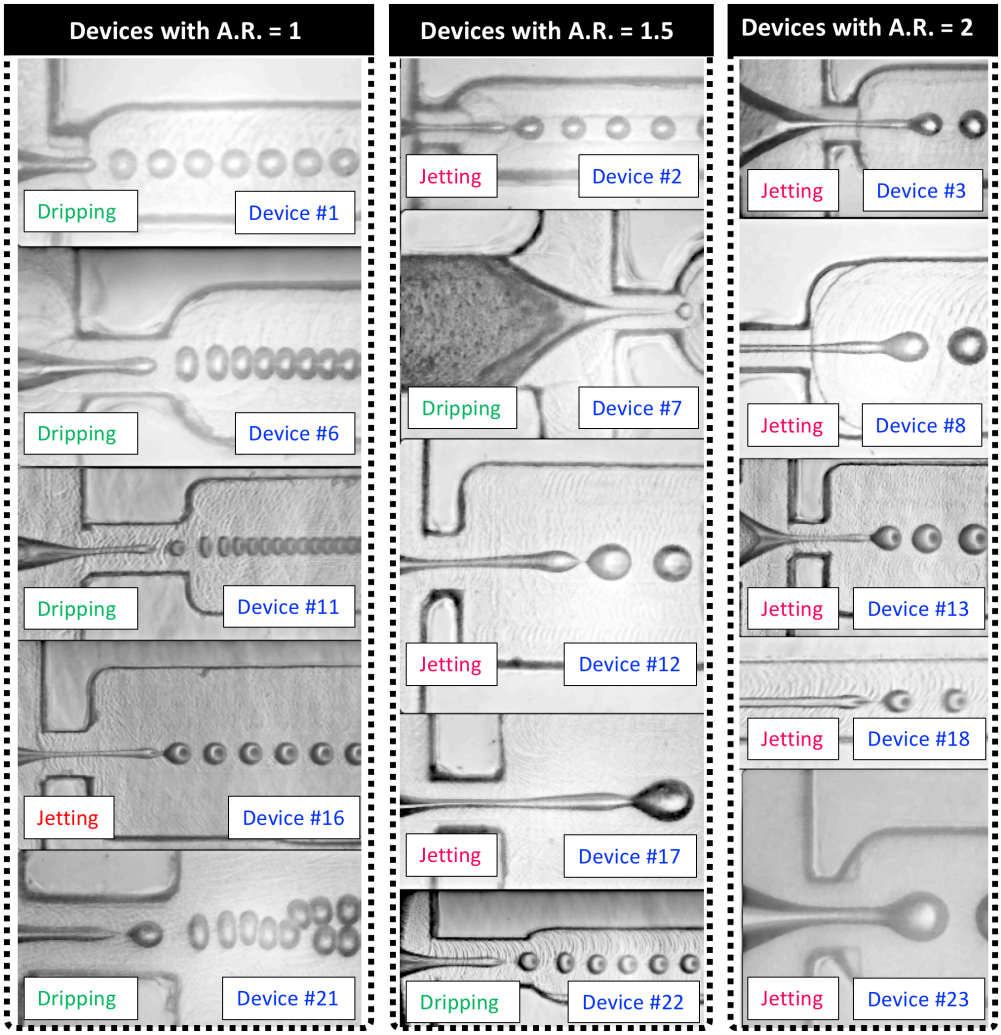

Figure S. 8 Effect of aspect ratio on the droplet formation regime. As the aspect ratio increases the chance of regime change from dripping to jetting at a constant flow condition increases. At a constant flow condition (i.e., $Ca. = 0.264$ & $\Phi = 16$) droplet formation occurred at the dripping regime in 4 out of 5 devices when aspect ratio was 1. At aspect ratio of 1.5 while keeping the same flow condition only 2 out of 5 devices generated droplets at the dripping regime. Finally, when aspect ratio was 2, at the same flow condition droplets were formed only at jetting regime

Therefore, aspect ratio plays a major role in all performance metrics of droplet generation at medium capillary numbers, where a regime change from dripping to jetting in expected. A smaller aspect ratio delays regime change to a higher capillary number, and a larger aspect ratio advances regime change to a lower capillary number. As explained in the manuscript increasing flow rate ratio and aspect ratio advances regime change to happen at lower capillary numbers as shown in Fig. S. 9.

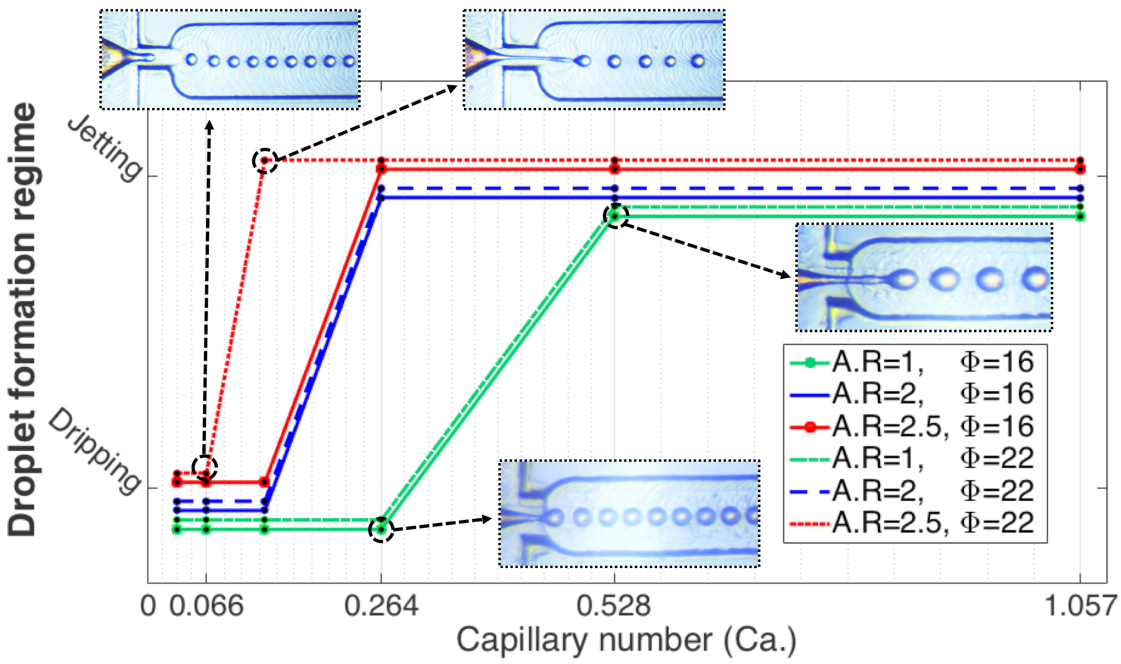

Figure S. 9. Effect of aspect ratio, flow rate ratio, and capillary number on generation regime. Lines not overlaid at dripping and jetting regimes for illustration purposes.

S. 5. 150 experimental data points of generation rate and droplet diameter

In here, we provided 150 of our experimentally measured data points on droplet generation rate and diameter. All the data points are given for a constant flow rate ratio of $\Phi = 10$. The data were categorized into five groups. The devices in each group have the same orifice width (i.e., 75, 100, 125, 150, & 175 µm), as shown in Fig. S. 10. The variations observed in these data points clarify the need of taking other geometric parameters into consideration while designing a microfluidic droplet generator. In the literature orifice width, capillary number, and flow rate ratio are typically discussed to control the performance of flow-focusing droplet generators. However, as demonstrated in Fig. S. 10 other geometric parameters are important as well. Using the data point provided here, and Fig. 4 and Fig. 5 of the manuscript, researchers can tune the performance of each device to meet an application-specific performance requirement. The two modes of behavior observed for both generation rate and droplet diameter are linked to two modes of droplet generation (i.e., dripping regime and jetting regime).

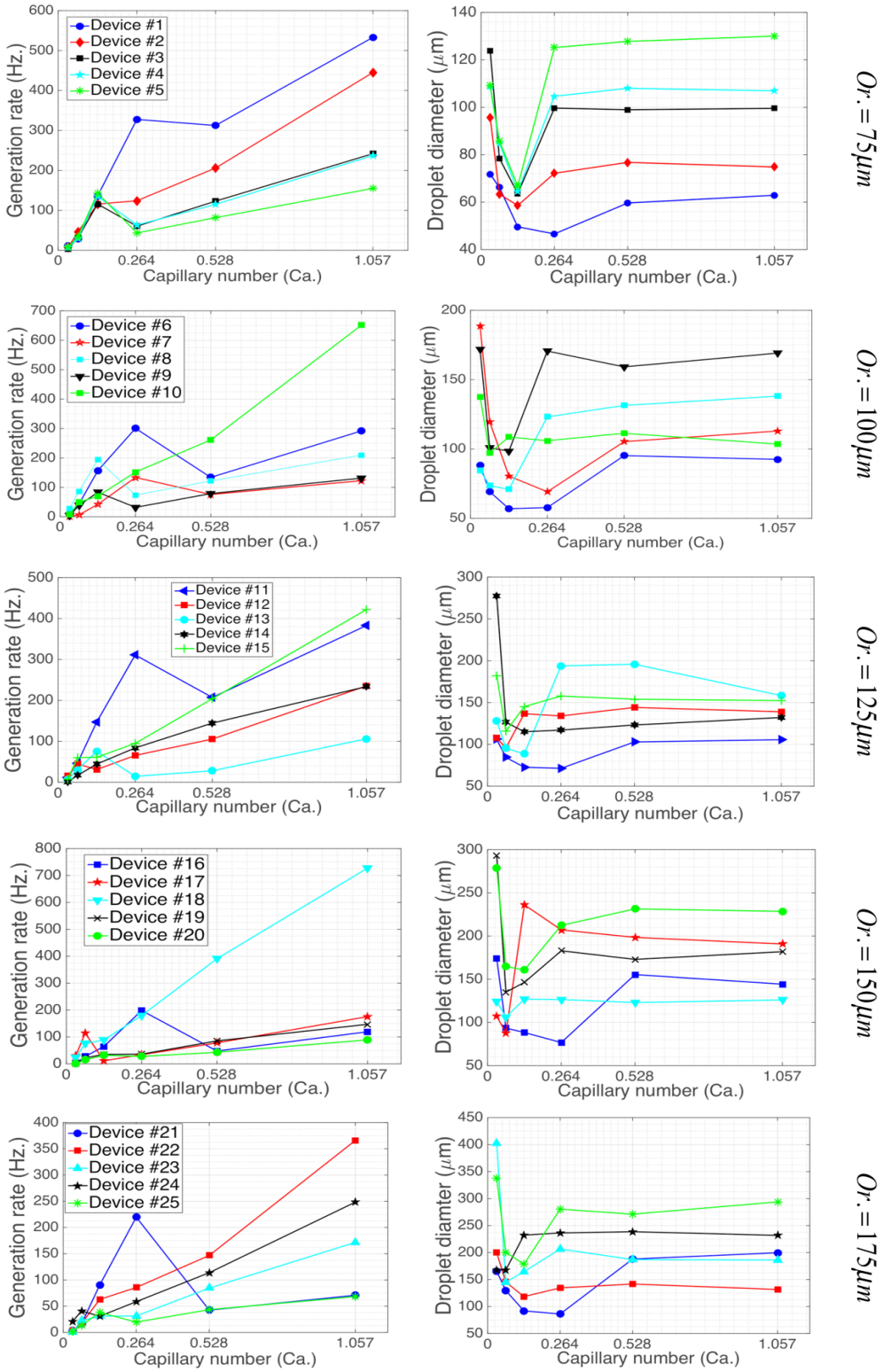

Figure S. 10. Variation of droplet generation rate and diameter with the capillary number for 25 devices at a constant flow rate ratio (i.e., Φ = 10). Devices have been categorized by orifice width, with each category including 5 devices. A total of 150 experimental data points are provided here. Researchers can use the data points shown here alongside information provided in Fig. 4 and Fig. 5 to further adjust the performance of droplet generation to achieve droplet formation with a size and a rate of interest.

S. 6. Application specific device selection

We also provided an easy way to choose a device based on the desired range of droplet diameter and generation rate, as shown in Table. S. 1. Droplet diameter and generation rate have been each categorized into 6 different groups, over the range of 0 – 400 µm and 0 – 800 Hz, respectively. It should be mentioned each device can deliver but is not limited the performance range given in Table. S. 1. Researchers can use the information provided in Fig. 4 – 7 of the manuscript to fine-tune any of the devices.

Table. S. 1. In this table, we suggest device numbers from the original 25 orthogonal devices of the study that can be used to deliver the desired range of droplet diameter and generation rate from 0- 400 µm and 0 - 800 Hz, respectively.

Droplet diameter / Generation rate	< 50 µm	50 – 100 µm	100 – 150 µm	150 – 200 µm	200 – 300 µm	300 – 400 µm
< 50 Hz.	1	1, 2, 3, 4, 5, 6, 7, 8, 9, 10, 11, 12, 13, 16, 17, 18, 19 & 21	3, 4, 5, 7, 9, 10, 11, 12, 13, 14, 15, 16, 17, 18, 19, 20, 21, 22, 23, 24, & 25	7, 9 13, 14, 15, 16, 17, 19, 20, 21, 22, 23, 24, & 25	14, 17, 19, 20, 22, 23, 24, & 25	23 & 25
50 – 100 Hz.	2	3, 4, 5, 7, 8, 9, 10, 11, 12, 13, 14, 15, 16, 17, 18, 19, 21, & 22	5, 7, 8, 9, 12, 14, 15, 16, 18, 19, & 22	9, 17, 19, 20, 21, 23, & 24	24 & 25	✗
100 – 200 Hz.	1, 2, 3, & 4	2, 3, 4, 5, 6, 7, 10, 11, 16, 17, 21, & 22	4, 5, 7, 8, 9, 11, 12, 13, 14, 15, 16, 18, 19, 22, & 23	17, 19, 23, & 24	24	✗
200 – 300 Hz.	1 & 6	2, 3, 4, 8, & 21	4, 8, 12, & 14	24	24	✗
300 – 500 Hz.	1 & 6	1, 2, 6, 10, 11, & 18	15, 18, & 22	✗	✗	✗
500 – 800 Hz.	1	1, 2, & 10	18	✗	✗	✗

S. 7. Overall parameter sensitivity of generation rate and droplet diameter

Finally, we ranked all the eight effective parameters in determining generation rate and droplet diameter in flow-focusing droplet generation using ANOVA method as shown in Fig. S. 11. It can be concluded that orifice length is the least significant geometric parameter in determining the performance of droplet generation.

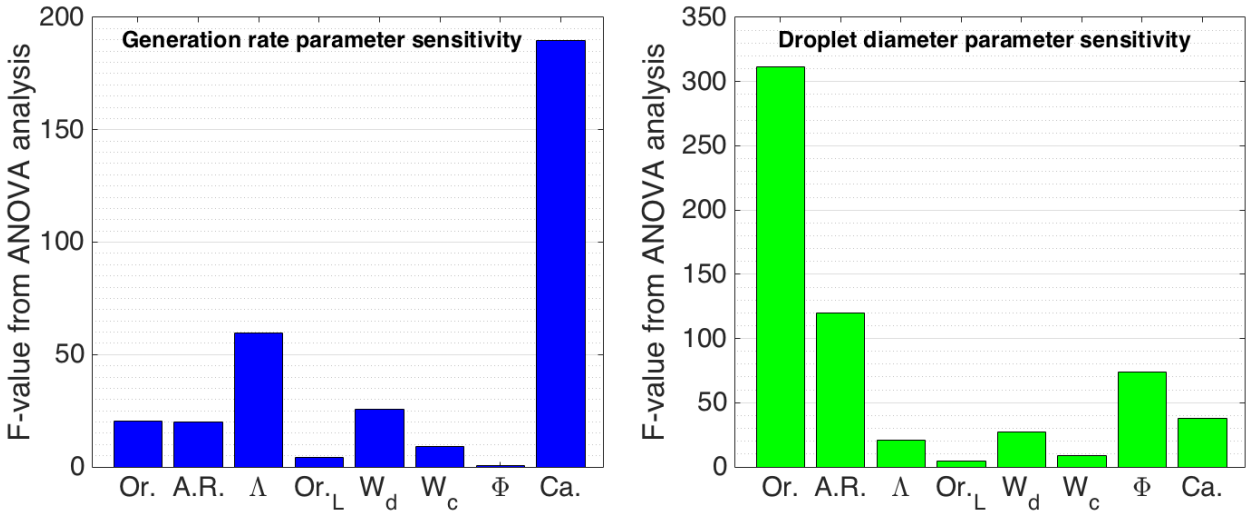

Figure S. 11 Overall significance of all the eight parameters affecting flow-focusing droplet generation, determined using ANOVA method.

S. 8. Algorithm to tune the droplet size

In order to help the researchers navigate through the findings of this paper easily, we provided a sample algorithm that could be used to fine-tune the droplet size based on the information provided in this study, as shown in A. 1. Based on the desired droplet size, the user can look up Table S. 1 to pick candidate devices that are able to deliver the desired droplet diameter. Then users can look up Fig. S. 10, to find the actual droplet diameter and the flow conditions that resulted in the observed diameter. If the actual droplet diameter value is not satisfactory, the user should identify the generation regime of the actual data point given in Fig. S. 10. This can be easily determined. If the data point is to the left of the smallest droplet diameter (for a single device) in the droplet diameter graphs of Fig. S. 10, the formation regime is dripping. If the data point is placed to the right of the smallest droplet diameter in the droplet diameter graphs of Fig. S. 10 the formation regime is jetting. Once, the formation regime is identified the percentage change required to achieve the desired droplet size must be calculated. If the required change is larger than 25% coarse-tuning is needed and if the change is smaller than 25% only fine-tuning is needed. Depending on whether coarse or fine tuning is needed, Fig. 5 (a) must be looked up to identify the coarse or fine tuners. Once the tuners are identified, depending on the formation regime Fig. S. 4 (for the dripping regime) or Fig. S. 6 (for the jetting regime) must be looked up to calculate what variations in the tuners will result in the desired percentage change in droplet diameter as shown below.

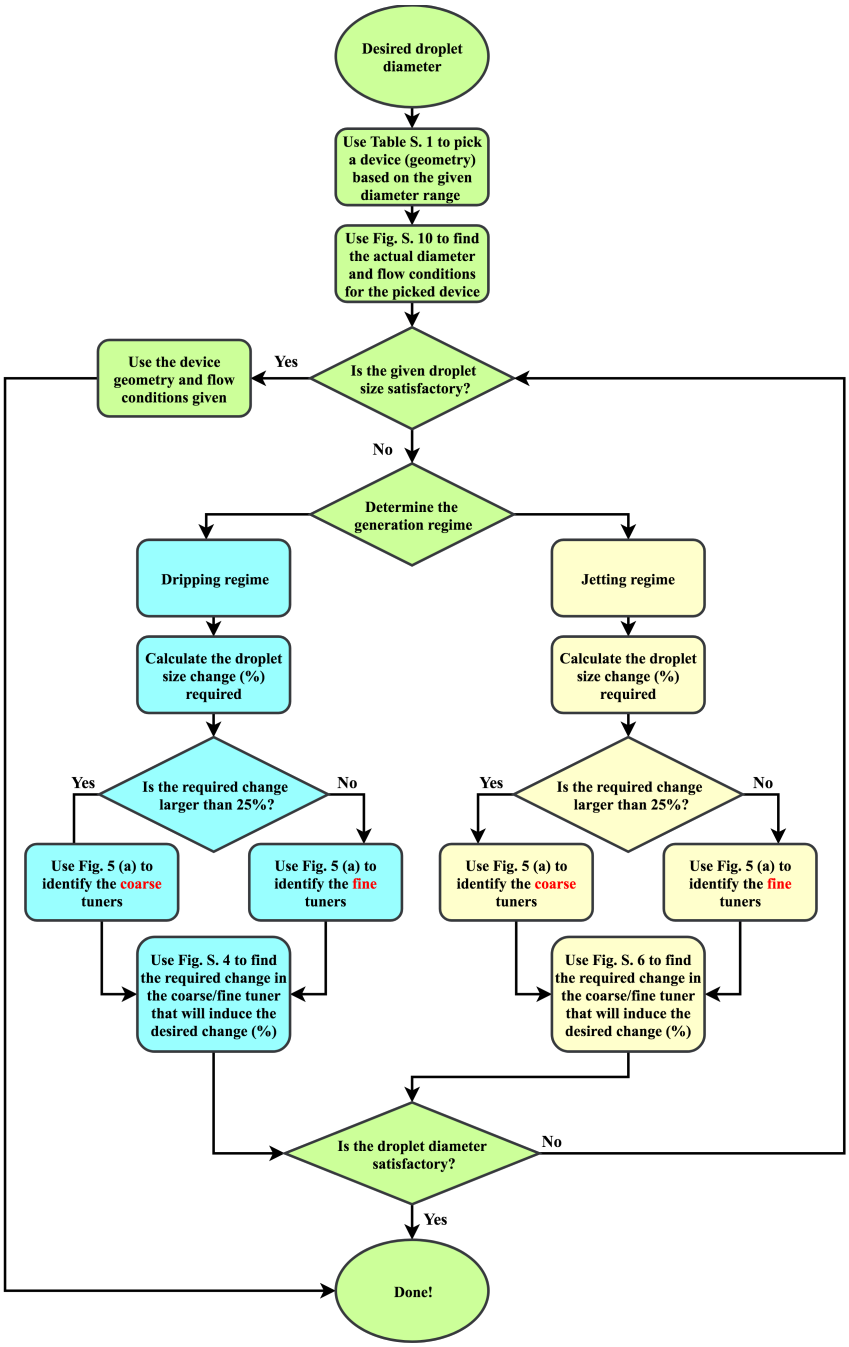

A. 1 Proposed algorithm to use the framework developed in this study to achieve a desired droplet size.

References

[1] Lashkaripour, Ali, Ryan Silva, and Douglas Densmore. "Desktop micromilled microfluidics." Microfluidics and Nanofluidics 22, no. 3 (2018): 31